Heavy Ion Test Report for the AD9364 RF Transceiver

Dakai Chen[1], Tim Mondy[2], and Anthony Phan[2]

1. NASA Goddard Space Flight Center, Greenbelt, MD 20771
2. ASRC Space & Defense, c.o. NASA Goddard Space Flight Center, Greenbelt, MD 20771

Test Date: March 17th, 2016

I. Introduction

The purpose of this test is to determine the heavy ion-induced single-event effect (SEE) susceptibility of the AD9364 from Analog Devices.

II. Device Under Test

The AD9364 is a high performance, highly integrated radio frequency (RF) Agile Transceiver designed for use in 3G and 4G base station applications. The device combines an RF front end with a flexible mixed-signal baseband section and integrated frequency synthesizers, simplifying design-in by providing a configurable digital interface to a processor. The AD9364 operates in the 70 MHz to 6.0 GHz range, covering most licensed and unlicensed bands. Channel bandwidths from less than 200 kHz to 56 MHz are supported. The device is built on a commercial 65 nm CMOS process. Therefore it is potentially susceptible to single-event latchup (SEL).

Figure 1 shows a functional block diagram of the device. Table I shows the basic part and test details. Detailed device parameters and functional descriptions can be found in the datasheet [1].

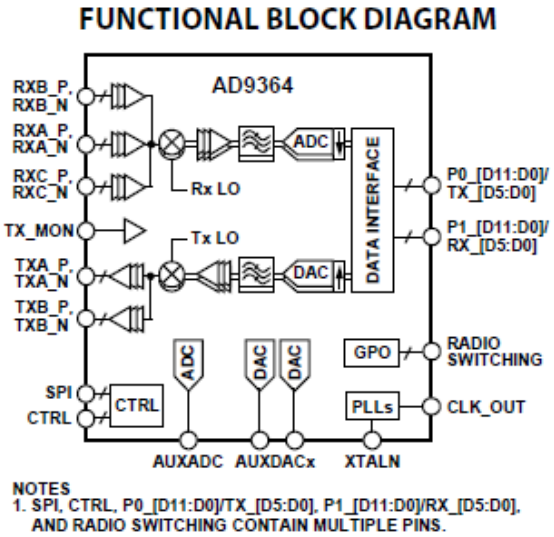

Figure 1. Schematic block diagram.

Table I
Part and test information.

Generic Part Number:	AD9364
Full Part Number	AD9364BBCZ
Manufacturer:	Analog Devices
Lot Date Code (LDC):	1401
Quantity Tested:	1
Serial Numbers of Control Sample:	TBD
Serial Numbers of Radiation Samples:	TBD
Part Function:	RF transceiver
Part Technology:	65 nm CMOS
Case Markings:	AD9364BBCZ #1401 2785560.1 SINGAPORE
Package Style:	144-Ball chip scale package ball grid array (CSP_BGA)
Test Equipment:	AD-FMCOMMS4-EBZ evaluation platform, ZedBoard, PC

III. Test Facility

The heavy-ion beam testing was carried out at the Texas A&M University Cyclotron Facility. The facility utilizes the K500 cyclotron with a superconducting magnet which generates the magnetic field used to accelerate the ions. The test setup was in an air environment.

Facility: Texas A&M University Cyclotron Facility
Cocktail: 15 MeV/nuc
Flux: 1×10^3 to 1×10^5 $cm^{-2} \cdot s^{-1}$
Fluence: up to 1×10^7 cm^{-2} (per run)
Ions: Shown in Table II

Table II.
Heavy-ion specie, linear energy transfer (LET) value, range, and energy.

Ion	Initial LET in air ($MeV \cdot cm^2/mg$)	Range in Si (µm)	Energy (MeV)
Ne	2.8	263	267
Ar	8.7	176	500
Cu	20.6	120	710
Xe	53.6	104	1316
Au	87.0	102	1294

IV. Test Method

A. *Test Setup*

The devices under test (DUT) were configured as a part of the AD-FMCOMMS4-EBZ evaluation platform, which constitutes the RF front end of a software defined radio (SDR). The AD-FMCOMMS4-EBZ is a high-speed 1 x 1 agile RF transceiver analog FPGA Mezzanine Card (FMC), software-tunable over the 56 MHz to 6 GHz band. The SDR system is a set of user tools running under a Linux operating system which allows the user to generate and receive RF waveforms. It is designed to operate with a FPGA evaluation board that supports the FMC interface and has the necessary fabric to support the Hardware Descriptive Language (HDL) requirement the SDR system and SD Card reader. The SDR system is provided by Analog Devices and loaded into the FPGA board using a specially configured SD-Card.

For this test, we used the ZedBoard to interface with the AD-FMCOMMS4-EBZ evaluation platform. The ZedBoard contains the Zynq-7020 System-on-Chip (SoC), 512 MB DDR3, 256 Mb Quad-SPI flash, and 4 GB SD memory card.

Figure 2 shows the top and bottom view of the evaluation board. The AD9364 is circled. As shown, there are several other active components mounted on the bottom of the board. These components are away from the DUT, so they were not exposed to the heavy ion beam. Figure 3 shows a photograph of the ZedBoard. The entire ZedBoard will be completely out of the beam line.

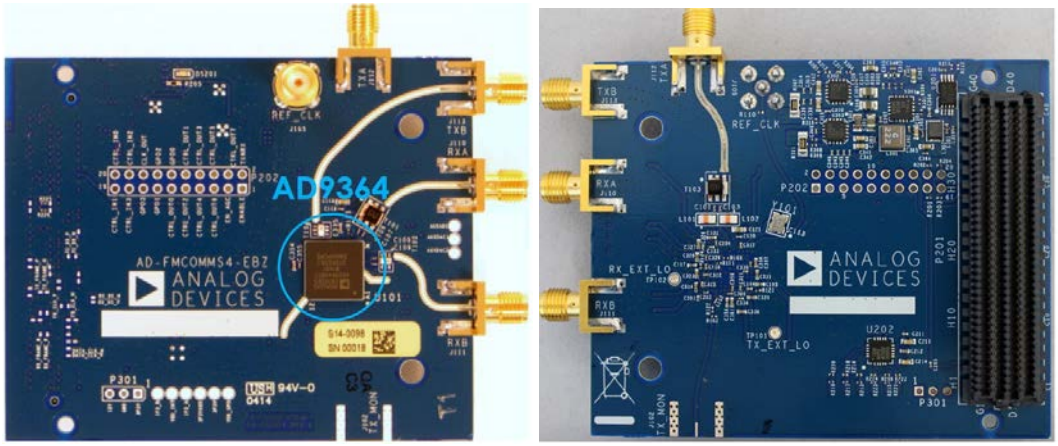

Figure 2. Top and bottom view of the AD-FMCOMMS4-EBZ evaluation board.

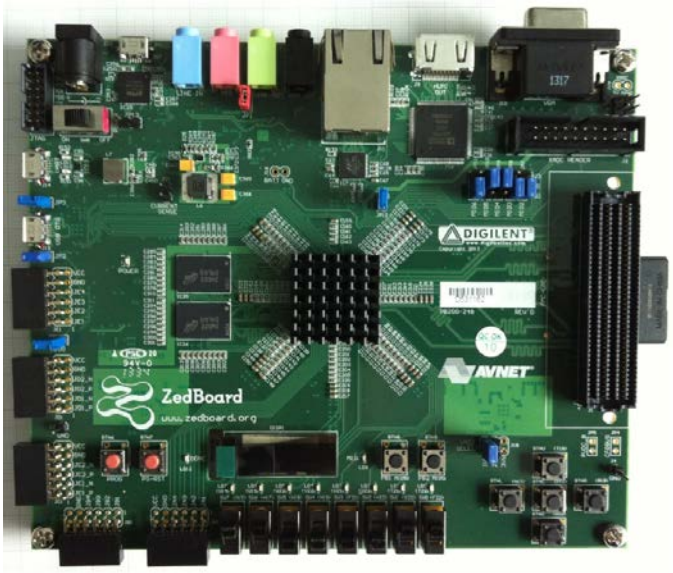

Figure 3. Photograph of the ZedBoard.

B. Irradiation procedure

We used a bit error rate program to evaluate the SEE susceptibility. The bit error rate tester generated a random data pattern. The data is transmitted in frames. The user PC carries out post-processing following transmission/reception of each frame. The radiation-induced errors were recorded during post processing. In addition, we continuously transmitted and received an image file during the irradiation.

We evaluated three data rates – 1.9, 15, and 31 Msample/sec. The transmission/reception time of each frame is fixed at 10 msec. So the amount of data transmitted/received per frame is proportional to the data rate. The data size per frame are 3.4, 270, and 550 kb for transmission rates of 1.9, 15, and 31 Msample/sec, respectively. Since it takes longer to process a larger frame, it follows that the resolution in the upset fluence becomes poorer for the higher data rates. As a result, we may underestimate the upset cross section for higher data rates.

The supply currents (main supply, interface, and GPO) were monitored throughout the test. In the event of a functional error, the operator first attempted to refresh the registers. If the part did not recover functionality, the operator power cycled the part.

C. Test Conditions

Test Temperature:	Ambient temperature (testing performed in vacuum)
Operating Frequency:	70 MHz to 6 GHz (internally driven)
Power Supply:	3.3 V
Angles of Incidence:	0^o (normal) to 60^o
Parameters:	1) Main supply voltage
	2) Main supply current
	3) GPO supply voltage
	4) GPO supply current

5) Interface supply voltage
6) Interface supply current
7) Output voltage
8) Frequency

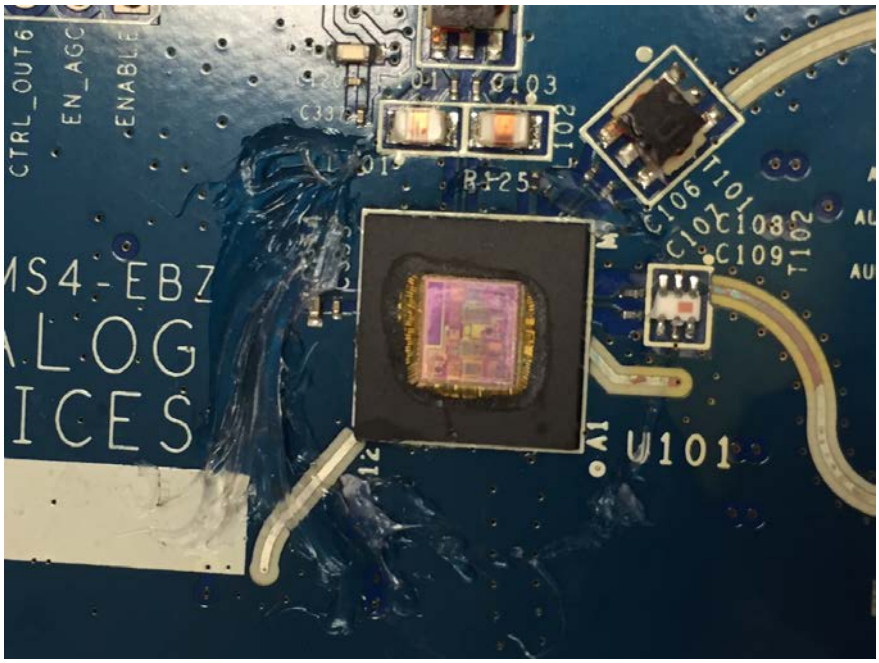

Figure 4. An acid-etched device with exposed die.

V. Results

We ran the majority of the test using the bit error tester program, in addition to one statically biased run. We also carried out several runs where we transmit and receive an image during irradiation. We found that the device is susceptible to single-event functional interrupts (SEFI). During a functional interrupt, half of the total number of bits read are errant. That is the most common type of SEFI. Another type of SEFI resulted in lost communication with the DUT. Recovery from functional interrupts require either reconfiguration of the device registers or power cycle. The device did not show single-event latchup or any other destructive effect up to a LET of 87 MeV·cm^2/mg for a fluence of 6.7 × 10^6 cm^{-2}, obtained with Au ions at normal incident. We tested one device.

Figure 5 shows the SEFI cross section for normal to 45^o, and 60^o incident irradiation angles. The LET threshold is below a LET of 2.8 MeV·cm^2/mg. We observed a sharp increase in cross section at 60^o incident angle relative to 45^o and 0^o.

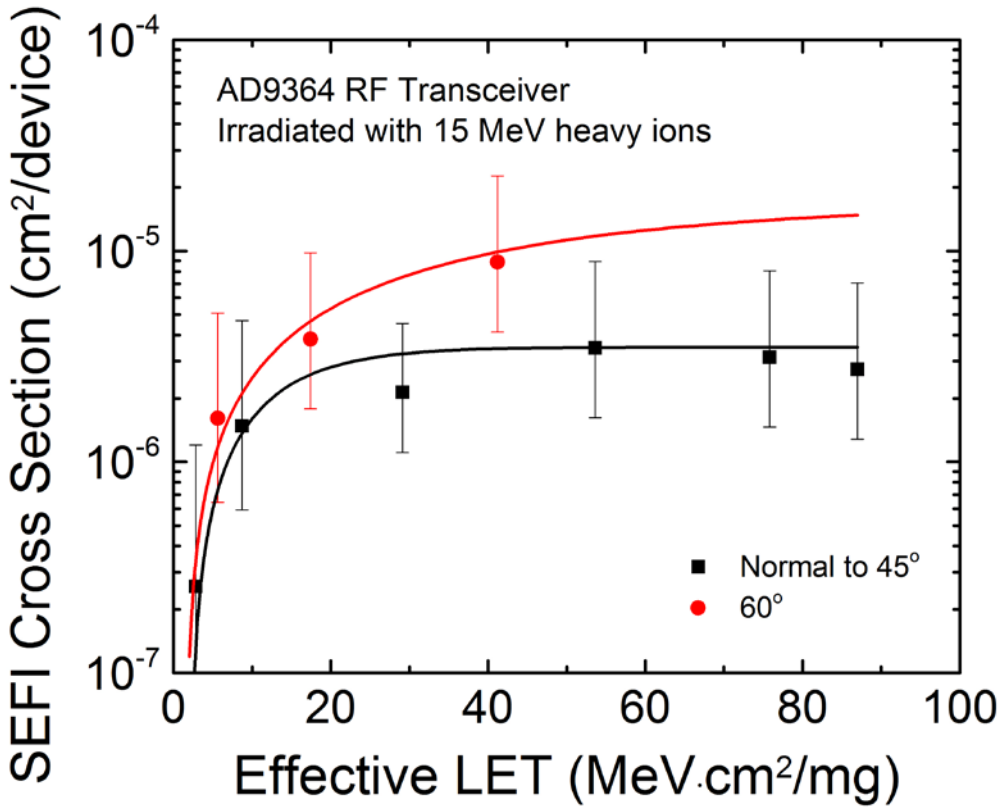

Figure 5. SEFI cross section vs. effective LET for the AD9364 irradiated with 15 MeV heavy ions. Error bars are Poisson errors at 95% confidence level.

A. Angular Dependence

Figure 6 compares the cross section at 60° with that at 45° and 0° for different LETs. The sets of data at each LET have the same data rate. We plot the cross section data from LETs closest to each other so they can provide meaningful comparison. The actual LET is shown above each column.

The figure shows that there is no enhancement from 0° to 45°, as illustrated by the data at LET of 30 and 81 MeV·cm^2/mg. There is sharp enhancement in the cross section at 60°. We did not test at an angle above 60°. The acute rise in cross section at 60° does not follow the cosine rule, which may suggest the presence of a thin and flat layer within or adjacent to the device sensitive layer stack. So the thin and flat sensitive volume layer is vulnerable to highly incident angle ions.

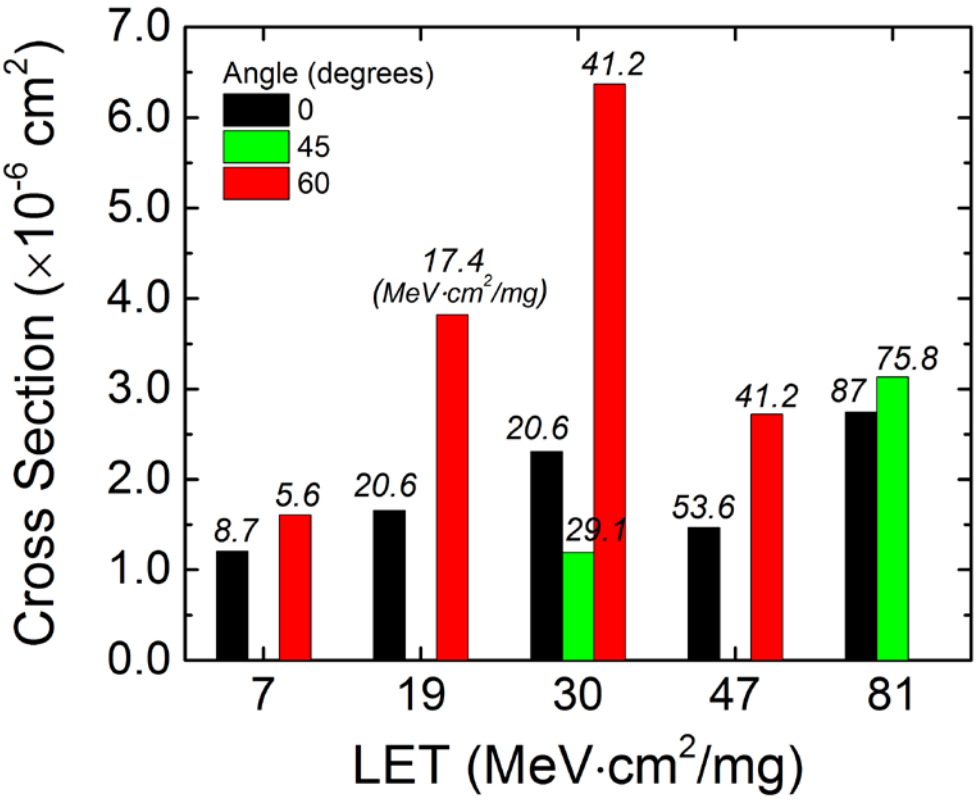

Figure 6. SEFI cross section vs. effective LET for different incident angles. At each LET, the cross section at 60º incident angle is compared with that at normal incident and/or 45º. The data at each LET have the same data rate. We plot the cross section from approximate LETs closest to each other so they can provide meaningful comparison. The actual LET is shown above each column.

Figure 7 shows the SEFI cross section as a function of data rate for various LETs. The data at an effective LET of 41.2 MeV·cm^2/mg was taken at 60º incident angle, while other data points are taken at 0º or 45º incident angle. The cross section generally decreases for increasing sample rate. We believe this is partly due to the lower measurement resolution at the higher sample rates, which resulted in a larger standard error by overestimating the time and fluence to upset. The size of the data package is smaller for a reduced transmission frequency. For example, we transmit/receive 3.4 kb per frame at 1.9 MS/sec, and 550 kb per frame at 31 MS/sec. The total data processing time is 1.4 sec per frame at 1.9 MS/sec vs. 13.9 sec per frame at 31 MS/sec. So we have higher measurement resolution for the fluence to SEFI at the lower transfer rate, since we perform characterization more frequently. Evidently, the cross section saturates at higher transmission speed, due the loss in resolution. The error bars shown in Figure 7 represent the upper bound cross section by taking into account the time lost during processing.

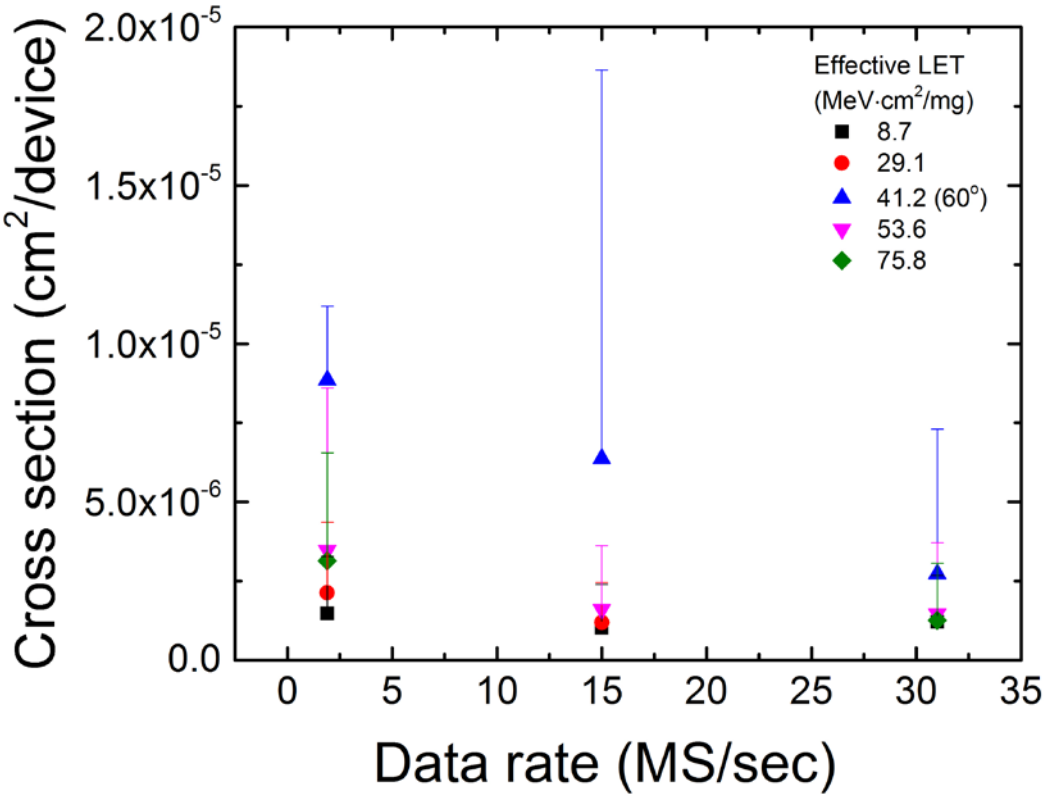

Figure 7. SEFI cross section vs. data rate for different LETs. Error bars represent upper bounds due to processing time. The data at an effective LET of 41.2 MeV·cm^2/mg was taken at 60^o incident angle, while other data points are taken at 0^o or 45^o incident angle.

B. Image Transfer

In addition to the bit error test, we also repeatedly transmit/receive an image during the irradiation. Figure 8 shows the before and after images for a SEFI. In this event, the SEFI wiped out two vertical stripes of pixels. Figure 9 shows the same before and after images for another SEFI, which had more significant impact. The image is not recognizable following this event.

Figure 8. Top image shows the pristine picture. Bottom image shows the picture after a SEFI.

Figure 9. Top image shows the pristine picture. Bottom image shows the picture after a SEFI.

C. SEFI Event Rate

Table II and Table III show the SEFI rates behind 100 mils of solid aluminum sphere in a geostationary orbit and a 675 km sun-synchronous low earth orbit. We show the event rate for 0º to 45º and for 60º incident angle. The cross section may be higher for angles greater than 60º. The protrusions from the board and the part package prevented

irradiation at higher angles. Table III shows the Weibull parameters used for the rate calculations.

Table II
SEFI event rate at 50% confidence level for 0º to 45º and 60º incident angle in a GEO orbit.

Incident Angle	0 to 45 degrees	60 degrees
100 mils Al	(#/day)	
Background	3.01×10^{-5}	6.26×10^{-5}
Worst Week	1.80×10^{-2}	7.10×10^{-2}

Table III
SEFI event rate at 50% confidence level for 0º to 45º and 60º incident angle in a 675 km sun-synchronous LEO orbit.

Incident Angle	0 to 45 degrees	60 degrees
100 mils Al	(#/day)	
Background	9.03×10^{-6}	1.91×10^{-5}
Worst Week	1.83×10^{-2}	7.13×10^{-2}

Table IV
Weibull parameters for 0º to 45º and 60º.

Parameter	0 to 45 degrees	60 degrees	Unit
LET_0	2.0	1.5	MeV·cm^2/mg
Sigma	3.5×10^{-6}	1.7×10^{-5}	cm^2
Exponent	1.2	1.1	*NA*
Width	12	45	MeV·cm^2/mg

VI. Reference

[1] Analog Devices, Inc. (2015, Nov.), "*AD9364 RF Agile Transceiver*" [Online]. Available: http://www.analog.com/media/en/technical-documentation/data-sheets/AD9364.pdf, Accessed on: Nov. 23, 2015.